Adhesion of membranes with competing specific and generic interactions

T.R. Weikl[1], D. Andelman[2], S. Komura[3], and R. Lipowsky[1]

[1] MPI für Kolloid- und Grenzflächenforschung, 14424 Potsdam, Germany
[2] School of Physics and Astronomy, Raymond and Beverly Sackler Faculty of Exact Sciences, Tel Aviv University, Tel Aviv 69978, Israel
[3] Department of Chemistry, Tokyo Metropolitan University, Tokyo 192-0397, Japan

Abstract. Biomimetic membranes in contact with a planar substrate or a second membrane are studied theoretically. The membranes contain specific adhesion molecules (stickers) which are attracted by the second surface. In the absence of stickers, the trans-interaction between the membrane and the second surface is assumed to be repulsive at short separations. It is shown that the interplay of specific attractive and generic repulsive interactions can lead to the formation of a potential barrier. This barrier induces a line tension between bound and unbound membrane segments which results in lateral phase separation during adhesion. The mechanism for adhesion-induced phase separation is rather general, as is demonstrated by considering two distinct cases involving: i) stickers with a linear attractive potential, and ii) stickers with a short-ranged square-well potential. In both cases, membrane fluctuations reduce the potential barrier and, therefore, decrease the tendency of phase separation.

PACS. 87.16.Dg Membranes, bilayers, and vesicles – 05.70.Np Interface and surface thermodynamics – 64.75.+g Solubility, segregation, and mixing; phase separation

1 Introduction

The adhesion of biomimetic membranes and vesicles is governed by various generic and specific interactions [1]. The simplest systems are provided by lipid bilayers which contain only one or a few lipid components and which have a laterally uniform composition. The generic interactions between one such membrane and another surface (or between two such membranes) can be of enthalpic or entropic origin.

The enthalpic contribution arises from the intermolecular forces such as hydration, van der Waals, and electrostatic forces. This contribution, called the direct membrane interaction, can be measured if the membrane is essentially flat or planar. Experimentally, a flat state can be prepared by immobilizing the membrane on a solid substrate. Theoretically, this state corresponds to the limit of a large membrane rigidity.

In aqueous solution, bilayer membranes are often quite flexible and then exhibit thermally-excited undulations which act to renormalize their direct interaction. If the direct interaction is purely repulsive, the undulations lead to a free-energy contribution which can be interpreted as an entropic or fluctuation-induced force as proposed in reference [2]. If the direct interaction contains an attrac-

tive potential well, the renormalized interaction leads to an unbinding transition as predicted in reference [3].

Biomembranes contain a large number of different lipids and anchored macromolecules. The attractive forces between two membranes are usually mediated by receptors or adhesion molecules which are anchored in the membranes [4–6]. These specific interactions govern the highly selective binding of cells which is essential for many biological processes such as immune response or tissue development [7]. From a theoretical point of view, the adhesive behavior of these rather complex biomembranes can be modelled, to a certain extent, by two-component membranes containing "generic" lipids and anchored stickers [8,9].

The interplay of generic and specific interactions has also been investigated experimentally. Adhesion-induced lateral phase separation into domains with small and large membrane separations has been found to occur in several biomimetic systems. The formation of blisters has been observed in membranes containing cationic lipids in contact with a negatively charged surface [10], and between membranes containing both negatively and positively charged lipids [11]. The coexistence of tight and weak adhesion states has been found for membranes with biotinylated lipids bound to another biotinylated surface *via* streptavidin [12], membranes with homophilic

csA-receptors from the slime mold *Dictyostelium discoideum* [13], and membranes containing specific ligands of integrin molecules adsorbed on a substrate [14]. Attractive membrane-mediated interactions between bound csA-receptors of adhering vesicles have been inferred from membrane tension jumps induced by the micropipet aspiration technique [15]. In addition to the receptors, the membranes studied in references [12–15] also contain repulsive lipopolymers to prevent non-specific adhesion. These observations indicate the existence of possible physical mechanisms for the aggregation of receptors in biological membranes which has been found during cell adhesion and results in the formation of focal contacts [7].

In this article, we present a detailed study of one possible mechanism for adhesion-induced phase separation concerning membranes with generic repulsive and specific attractive interactions. For these membranes, tracing over the sticker degrees of freedom in the partition function leads to an effective trans-membrane interaction which exhibits a potential barrier. Such trans-membrane interactions have been previously studied in references [16, 17]. The phase separation results from the line tension between bound and unbound membrane regions due to this potential barrier. Membrane fluctuations reduce the barrier and, therefore, decrease the tendency for phase separation. The mechanism is thus clearly distinct from entropic, fluctuation-induced mechanisms for adhesion-induced phase separation as discussed in references [9,18]. Similar mechanisms for phase separation due to an effective potential barrier have also been studied recently in references [9,19,20].

The mechanism studied here is rather general as will be demonstrated by considering two different cases. In the first case, we assume that the generic trans-membrane interaction is repulsive for short separations and attractive for large separations. The generic trans-interaction is then approximated by a harmonic potential centered at the potential minimum at $l = l_0$. The specific trans-interaction is expanded up to linear order in $l - l_0$, and can be thought to arise from restoring forces of extensible sticker molecules which are irreversibly bound to the membrane and the substrate. In the absence of membrane shape fluctuations, the lateral phase behavior can be determined exactly. Using Monte Carlo simulations, we furthermore show that the membrane fluctuations reduce the potential barrier and the tendency for lateral phase separation.

In the second case, we consider a generic trans-membrane repulsion which is modeled as a square-barrier potential. In addition, the trans-interaction of the stickers is modeled as a square-well potential [8,9,18]. The stickers are bound for small separations from the substrate, and unbound otherwise. The square-well potential is a simple model for short-ranged lock-and-key interactions of ligands and receptors. After partial summation over the sticker degrees of freedom, we find again an effective potential barrier if the generic repulsion is longer ranged than the specific attraction of the stickers. As in the first case, this barrier leads to lateral phase separation, and is effectively reduced by membrane fluctuations.
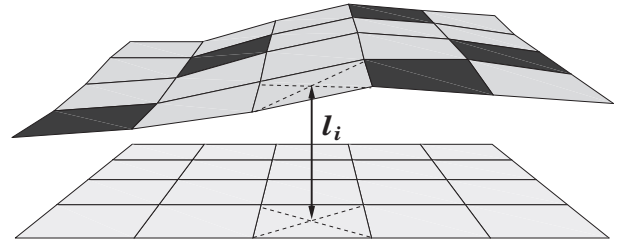

Fig. 1. A membrane segment consisting of 5×4 membrane patches in contact with another planar surface. The patches are labeled by the lattice sites i. The local separation of the membrane from the reference plane is denoted by l_i. The composition of the membrane is described by occupation numbers $n_i = 0$ and $n_i = 1$ corresponding to grey patches with no sticker and black patches with one sticker, respectively.

2 The model

A systematic description of a biomimetic membrane with stickers in contact with a substrate or a second membrane has to include a field $l(x, y)$ for the local separation of the membrane(s) and a concentration field $n(x, y)$ of the stickers above a position (x, y) on a reference plane. In the following, we apply a theoretical framework which has been introduced in reference [8] and extended in references [9,18]. Within this framework, the membrane is divided into small patches with a linear size a which corresponds to the smallest possible wavelength for bending deformations. According to computer simulations for molecular membranes, this size is about 6 nm for lipid bilayers with a thickness of about 4 nm [21]. For a membrane which is on average parallel to a planar substrate, this leads to an effective discretization of the reference plane into a two-dimensional square lattice with lattice parameter a. The sticker positions are described by occupation numbers $n_i = 0$ or 1 where $n_i = 1$ indicates the presence of a sticker at lattice site i, and the local separation is given by $l_i \geq 0$ [8], see Figure 1. An alternative continuous Ginzburg-Landau theory for the sticker concentration field was used in reference [19].

In terms of these variables, the grand canonical Hamiltonian has the general form

$$\mathcal{H}\{l, n\} = \mathcal{H}_{\mathrm{el}}\{l\} + \sum_i \left[V_{\mathrm{g}}(l_i) + n_i \left(V_{\mathrm{s}}(l_i) - \mu \right) \right], \quad (1)$$

where the elastic term

$$\mathcal{H}_{\mathrm{el}}\{l\} = \sum_i \frac{\kappa}{2a^2} (\Delta_{\mathrm{d}} l_i)^2 \quad (2)$$

represents the discretized bending energy of the membrane with bending rigidity κ, and the discretized Laplacian Δ_{d} is given by

$$\begin{aligned} \Delta_{\mathrm{d}} l_i = \Delta_{\mathrm{d}} l(x, y) &= l(x + a, y) + l(x - a, y) \\ &+ l(x, y + a) + l(x, y - a) - 4l(x, y). \end{aligned} \quad (3)$$

The term $(\Delta_{\mathrm{d}} l_i)^2$ corresponds to the leading-order expression for the mean curvature squared of a membrane with

vanishing spontaneous curvature [22,23]. The second term of the Hamiltonian (1) contains i) the generic interaction potential $V_{\mathrm{g}}(l)$ between the membrane and substrate and ii) the specific adhesion potential $V_{\mathrm{s}}(l)$ of the stickers which only contributes at lattice sites with $n_i = 1$, *i.e.* at lattice sites where stickers are present. The relative chemical potential of the stickers is denoted by μ. The same description holds for a multicomponent membrane in contact with a second, homogeneous membrane. In the latter case, the effective bending rigidity κ is given by $\kappa_1\kappa_2/(\kappa_1 + \kappa_2)$, where κ_1 and κ_2 denote the bending rigidities of the two membranes [24].

Note that $V_{\mathrm{g}}(l)$ and $V_{\mathrm{s}}(l)$ are the interaction energies *per membrane patch* where each patch has area a^2. Thus, the interaction energies per unit area are given by $V_{\mathrm{g}}(l)/a^2$ and $V_{\mathrm{s}}(l)/a^2$, respectively. This differs from the convention in reference [8], where the interaction potentials were defined as energies per unit area.

In the following, we neglect direct interactions between pairs of stickers which can be described by quadratic terms in the concentration field n [9,18]. The Hamiltonian (1) is then linear in n, and the sticker degrees of freedom in the partition function

$$\mathcal{Z} = \left[\prod_i \int_0^\infty \mathrm{d}l_i\right]\left[\prod_i \sum_{n_i=0,1}\right]\exp\left[-\frac{\mathcal{H}\{l,n\}}{T}\right] \quad (4)$$

can be partially summed or traced over exactly, leading to

$$\mathcal{Z} = \left[\prod_i \int_0^\infty \mathrm{d}l_i\right]\exp\left[-\frac{\mathcal{H}_{\mathrm{el}}\{l\} + \sum_i V_{\mathrm{ef}}(l_i)}{T}\right] \quad (5)$$

with the effective potential

$$V_{\mathrm{ef}}(l) = V_{\mathrm{g}}(l) - T\ln\left(1 + \exp\left[\frac{\mu - V_{\mathrm{s}}(l)}{T}\right]\right), \quad (6)$$

where T denotes the temperature in energy units (*i.e.*, the Boltzmann constant k_{B} is absorbed into the symbol T). The partial summation over the sticker degrees of freedom $\{n\}$ thus leads to an equivalent problem of a laterally *homogeneous* membrane with the effective potential (6).

3 Linear sticker potential

In this section, we consider a generic potential V_{g} between the membrane and the substrate which has a relatively deep minimum at a certain separation l_0 from the substrate. Such a potential arises, *e.g.*, for electrically neutral surfaces interacting *via* strong van der Waals forces. Using a Taylor expansion around the minimum, we approximate this generic potential by the harmonic potential

$$V_{\mathrm{g}}(l) = \frac{v_2}{2a^2}(l - l_0)^2, \quad (7)$$

where $v_2 = a^2(\mathrm{d}^2V_{\mathrm{g}}/\mathrm{d}l^2)|_{l_0}$.

In addition to this generic potential, we consider extensible sticker molecules which are irreversibly bound to both the substrate and the membrane, and which have an unstretched extension small compared to l_0. We will further assume that the corresponding sticker potential $V_{\mathrm{s}}(l)$ has an essentially constant gradient for those values of l for which we can use the harmonic approximation (7) for the generic potential. In such a situation, we may truncate the expansion of the sticker potential in powers of $l - l_0$ and use

$$V_{\mathrm{s}}(l) = V_{\mathrm{s}}(l_0) + \frac{\alpha(l - l_0)}{a}, \quad (8)$$

with $\alpha \equiv a\partial V_{\mathrm{s}}(l)/\partial l|_{l_0} > 0$.

In order to simplify the notation and to reduce the number of parameters, it is convenient to introduce the rescaled variables

$$h \equiv \sqrt{\frac{v_2}{T}}\,\frac{l - l_0}{a}. \quad (9)$$

The Hamiltonian (1) with the generic potential (7) and the specific potential (8) can then be written as

$$\frac{\mathcal{H}\{h,n\}}{T} = \sum_i \left[\frac{\kappa}{2v_2}(\Delta_{\mathrm{d}}h_i)^2 + \frac{1}{2}h_i^2 + n_i(\tilde{\alpha}h_i - \tilde{\mu})\right] \quad (10)$$

in terms of the discrete lattice variables h_i, n_i, and the dimensionless parameters

$$\tilde{\alpha} = \frac{\alpha}{\sqrt{v_2 T}} \quad\text{and}\quad \tilde{\mu} = \frac{\mu - V_{\mathrm{s}}(l_0)}{T}, \quad (11)$$

and the effective potential (6) has the form

$$\frac{V_{\mathrm{ef}}(h)}{T} = \frac{1}{2}h^2 - \ln\left(1 + e^{\tilde{\mu} - \tilde{\alpha}h}\right). \quad (12)$$

Direct inspection of these equations shows that the system considered here depends on three dimensionless parameters: i) the reduced coupling constant $\tilde{\alpha}$ of the specific potential, ii) the reduced (and shifted) chemical potential $\tilde{\mu}$, and iii) the ratio κ/v_2 of the bending rigidity κ and the strength v_2 of the generic harmonic potential (7).

3.1 Limit of rigid membranes

For large values of the ratio κ/v_2, thermally excited shape fluctuations of the membrane can be neglected. The free energy $F = -(T/A)\ln\mathcal{Z}$ per area A is then given by V_{ef}/a^2. The phase behavior is determined by the minimization of the effective potential (12):

$$\frac{\partial V_{\mathrm{ef}}}{\partial h} = 0. \quad (13)$$

First-order phase transitions are found when different minima of V_{ef} coexist.

For the effective potential (12), the discussion of the phase behavior is simplified if this potential is expressed in terms of the shifted separation field

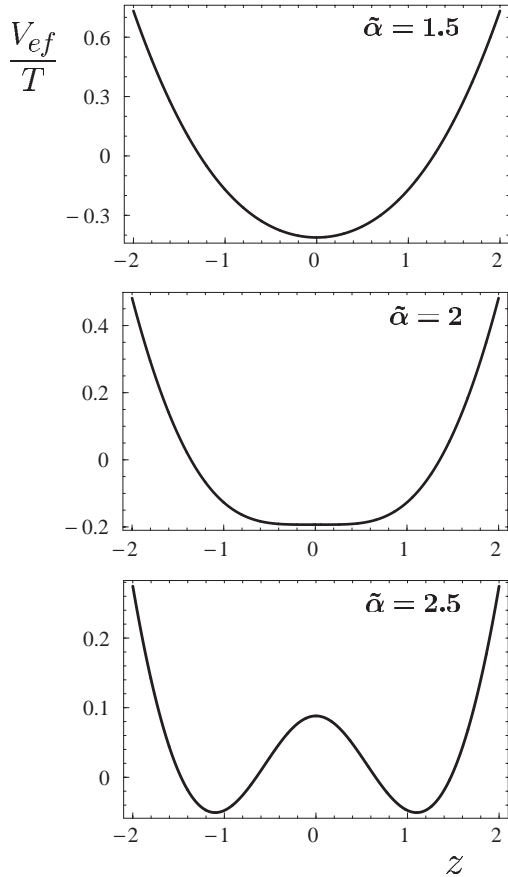$$z \equiv h + \tilde{\alpha}/2. \quad (14)$$

Fig. 2. The effective potential V_{ef} as a function of the shifted separation variable z for three values of the coupling $\tilde{\alpha}$. The analytical expression for V_{ef} is given in (16). For small and large values of $\tilde{\alpha}$, V_{ef} exhibits a single minimum and two degenerate minima, respectively, as shown in the top and bottom parts. At $\tilde{\alpha} = \tilde{\alpha}_c = 2$, the potential has the shape shown in the middle and undergoes a continuous bifurcation.

For the special line in the $(\tilde{\mu}, \tilde{\alpha})$ parameter space as given by

$$\tilde{\mu} = \tilde{\mu}_* \equiv -\tilde{\alpha}^2/2 \,, \tag{15}$$

the effective potential (12) has the form

$$\left. \frac{V_{\text{ef}}(z)}{T} \right|_{\tilde{\mu}=\tilde{\mu}_*} = \frac{z^2}{2} + \frac{\tilde{\alpha}^2}{8} - \ln\left[2\cosh(\tilde{\alpha} z/2) \right] \tag{16}$$

which is symmetric under the inversion $z \to -z$.

As one varies the parameter $\tilde{\alpha}$ while keeping $\tilde{\mu} = \tilde{\mu}_*(\tilde{\alpha})$, the effective potential given by (16) undergoes a continuous bifurcation at the critical value $\tilde{\alpha} = \tilde{\alpha}_c = 2$, see Figure 2. For $\tilde{\alpha} < \tilde{\alpha}_c$ and $\tilde{\alpha} > \tilde{\alpha}_c$, this potential has a single minimum at $z = 0$ and two degenerate minima at finite values of z, respectively. The critical value $\tilde{\alpha}_c = 2$ of the bifurcation point can be directly inferred from the second derivative of (16) as given by

$$\left. \frac{1}{T} \frac{\mathrm{d}^2 V_{\text{ef}}(z)}{\mathrm{d} z^2} \right|_{\tilde{\mu}=\tilde{\mu}_*} = 1 - \frac{\tilde{\alpha}^2}{4\cosh^2(\tilde{\alpha} z/2)} \,. \tag{17}$$

For $z = 0$, this expression is equal to $1 - \tilde{\alpha}^2/4$ which vanishes for $\tilde{\alpha} = \tilde{\alpha}_c = 2$. In the limit of rigid membranes as

considered here, one can ignore the effect of membrane fluctuations and the bifurcation point of the effective potential is identical with the critical point of the system which thus lies at $\tilde{\alpha}_c = 2$ and $\tilde{\mu}_c = -\tilde{\alpha}_c^2/2 = -2$.

Thus, for $\tilde{\mu} = \tilde{\mu}_*(\tilde{\alpha})$ and $\tilde{\alpha} > 2$, the effective potential (12) is a symmetric double-well potential with two degenerate minima. As soon as the chemical potential $\tilde{\mu}$ deviates from its coexistence value $\tilde{\mu} = \tilde{\mu}_*$, this symmetry is broken and the effective potential exhibits a unique global minimum. Therefore, the system undergoes a discontinuous transition as one changes the chemical potential from $\tilde{\mu} = \tilde{\mu}_* - \epsilon$ to $\tilde{\mu} = \tilde{\mu}_* + \epsilon$ for $\tilde{\alpha} > 2$, where ϵ denotes a small chemical potential difference.

The positions, say z_0, of the extrema of the effective potential are determined by $\mathrm{d} V_{\text{ef}}(z)/\mathrm{d} z = 0$. Along the coexistence line given by $\tilde{\mu} = \tilde{\mu}_* = -\tilde{\alpha}^2/2$, this leads to the transcendental equation

$$z_0 = \frac{\tilde{\alpha}}{2} \tanh\left(\frac{\tilde{\alpha} z_0}{2} \right) \,. \tag{18}$$

This equation has the trivial solution $z_0 = 0$ for all values of $\tilde{\alpha}$ which corresponds to a minimum and maximum for $\tilde{\alpha} < \tilde{\alpha}_c = 2$ and $\tilde{\alpha} > \tilde{\alpha}_c = 2$, respectively. For $\tilde{\alpha} > \tilde{\alpha}_c = 2$, equation (18) has two additional solutions corresponding to the two degenerate minima of the effective potential V_{ef}, see Figure 2.

For rigid membranes with large κ/v_2, the sticker concentration $X \equiv \langle n_i \rangle / a^2$ is given by

$$X = -\frac{\partial F}{\partial \mu} = -\frac{1}{a^2} \frac{\partial V_{\text{ef}}}{\partial \mu} = \frac{1}{a^2} \frac{e^{\tilde{\mu} - \tilde{\alpha} y_0}}{1 + e^{\tilde{\mu} - \tilde{\alpha} y_0}} \tag{19}$$

with $y_0 \equiv z_0 - \tilde{\alpha}/2$ which denotes the position of the minima of the effective potential (12). Along the coexistence line with $\tilde{\mu} = \tilde{\mu}_* = -\tilde{\alpha}^2/2$, this expression simplifies and becomes

$$\left. X \right|_{\tilde{\mu}=\tilde{\mu}_*} = \frac{1}{a^2} \frac{e^{-\tilde{\alpha} z_0}}{1 + e^{-\tilde{\alpha} z_0}} \,. \tag{20}$$

Inserting the numerically determined solutions of the transcendental equation (18) into (20) leads to the concentrations of the coexisting phases which determine the phase diagram shown in Figure 3. Inside the shaded two-phase region, a sticker-poor phase characterized by a relatively large separation y_0 of the membrane from the substrate coexists with a sticker-rich phase with a relatively small value of y_0.

3.2 Flexible membranes

For a fluctuating membrane in a symmetric double-well potential, first-order transitions only exist if the barrier between the two potential wells exceeds a certain critical height [16,17]. For barrier heights below this critical value, the fluctuating membrane "tunnels" through the barrier and there is no phase transition. Therefore, the critical point of a flexible membrane in the double-well potential (16) will be characterized by reduced coupling constants
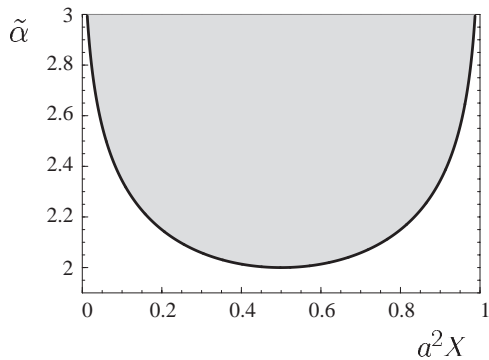
Fig. 3. Phase diagram for linear stickers in the absence of membrane fluctuations, depending on the sticker concentration X and the reduced coupling constant $\tilde{\alpha}$. Within the grey two-phase region, a sticker-poor phase characterized by a relatively large membrane-surface separation coexists with a sticker-rich phase for which this separation is relatively small. The critical point is located at $a^2 X_c = 1/2$ and $\tilde{\alpha}_c = 2$.

$\tilde{\alpha}_c = \tilde{\alpha}_c(\kappa/v_2)$ which exceed the bifurcation value $\tilde{\alpha}_c = 2$ as obtained for rigid membranes in the limit of large κ/v_2.

Using Monte Carlo simulations, the critical point can be determined, for a fixed value of κ/v_2, from an evaluation of the moments

$$C_2 = \frac{\langle \bar{z}^2 \rangle}{\langle |\bar{z}| \rangle^2} \quad \text{and} \quad C_4 = \frac{\langle \bar{z}^4 \rangle}{\langle \bar{z}^2 \rangle^2}, \quad (21)$$

where

$$\bar{z} = \frac{1}{N} \sum_{i=1}^{N} z_i \quad (22)$$

is the spatially averaged order parameter, and $\langle \cdots \rangle$ denotes averages over all membrane configurations [17,25]. For $\tilde{\alpha} > \tilde{\alpha}_c$ and correlation lengths ξ which are much smaller than the linear size L of the finite membrane, the moments reach the values $C_2 = 1$ and $C_4 = 1$, whereas for $0 < \tilde{\alpha} < \tilde{\alpha}_c$ and $\xi \ll L$, we have $C_2 = \pi/2 \approx 1.57$ and $C_4 = 3$. For $L \ll \xi$ on the other hand, the moments C_2 and C_4 vary only weakly with the linear size L. The critical value $\tilde{\alpha}_c$ of the reduced coupling constant can then be estimated from the common intersection point of C_2 and C_4, respectively, as a function of $\tilde{\alpha}$ for several values of L [17,25], see Figure 4.

In Figure 5, we display the obtained values for the critical rescaled coupling constant $\tilde{\alpha}_c$ as a function of the reduced rigidity κ/v_2. For large κ/v_2, $\tilde{\alpha}_c$ approaches the limiting value $\tilde{\alpha}_c = 2$ which is appropriate for rigid membranes as discussed in the previous section. As one decreases κ/v_2, the membrane fluctuations become more pronounced and act to increase the value of $\tilde{\alpha}_c$. This implies that the wells of the effective potential (16) have a finite depth as one reaches the critical point of the system.

Lateral phase separation occurs for coupling constants $\tilde{\alpha} > \tilde{\alpha}_c$. In either of the two phases, the entire membrane is located around one of the minima in the effective potential. In the sticker-poor phase, the membrane is found in the minimum with larger separation y_0 from the substrate.
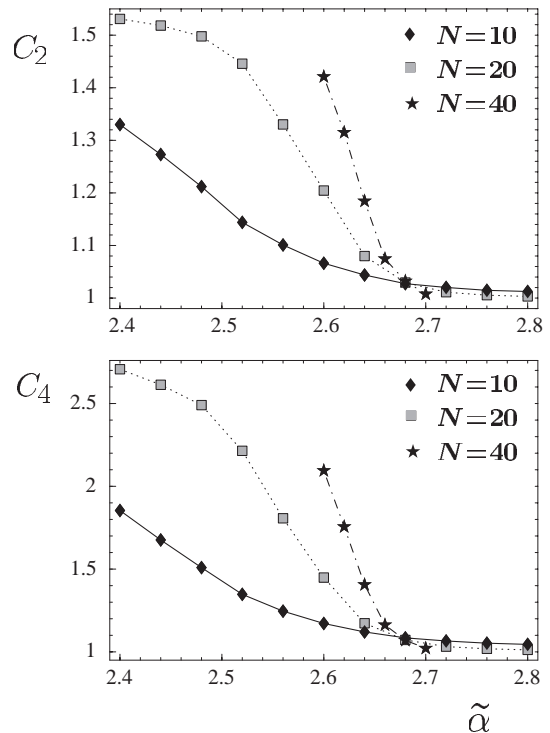

Fig. 4. Monte Carlo data for the moments C_2 and C_4 defined in (21) as a function of the reduced coupling constant $\tilde{\alpha}$. The ratio of the bending rigidity κ and of the strength v_2 for the generic harmonic potential (7) has the fixed value $\kappa/v_2 = 1$. The membrane segments studied in the simulations consist of $N \times N$ membrane patches.
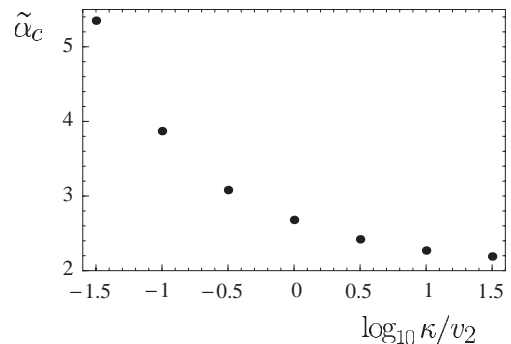

Fig. 5. The critical values $\tilde{\alpha}_c$ of the reduced coupling constant $\tilde{\alpha}$ as a function of the reduced membrane rigidity κ/v_2. The reduced coupling constant $\tilde{\alpha}$ is defined in (11) and governs the strength of the linear sticker potential as given by (8). For large values of κ/v_2, one attains the limit of rigid membranes with $\tilde{\alpha}_c \approx 2$. The statistical errors are smaller than the size of the symbols.

This minimum is dominated by the generic membrane potential and corresponds to a state of weak adhesion. In the sticker-rich phase, the membrane fluctuates around the minimum with smaller separation y_0 corresponding to a state of tight adhesion. In contrast, there is only a single phase for coupling constants $\tilde{\alpha} < \tilde{\alpha}_c$. For example, for $2 < \tilde{\alpha} < \tilde{\alpha}_c$ the two minima of the effective potential are both populated by many different segments of the

fluctuating membrane which is able to cross the potential barrier between the minima.

4 Square-well sticker potential

Let us now turn to stickers with a specific adhesion potential

$$V_s(l) = U\theta(l_v - l) = U, \quad \text{for} \quad 0 \le l \le l_v,$$
$$= 0, \quad \text{for} \quad l > l_v, \tag{23}$$

where $\theta(x)$ is the Heaviside function $\theta(x) = 0$ for $x < 0$ and $\theta(x) = 1$ for $x \ge 0$. The parameter U has the same dimension as the membrane potential V_s and represents the interaction energy per sticker.

Stickers which interact *via* the square-well potential (23) can attain two different states: A bound state with binding energy $U < 0$ if the local separation l between the membrane and the substrate is smaller than the potential range l_v, and an unbound state otherwise. Because the fluctuating membrane cannot penetrate the substrate surface, the membrane separations l are restricted to non-negative values. In contrast to the linear sticker potential of the previous section with the specific potential (8), the stickers characterized by the interaction potential (23) have a fixed length and cannot be stretched. Thus, the square-well potential as given by (23) provides a simple model for short-range interactions arising, *e.g.*, from specific ligand/receptor lock-and-key interactions or from screened electrostatic forces for charged stickers in contact with an oppositely charged substrate.

The phase behavior of multicomponent membranes containing stickers which interact *via* the square-well potential as given in (23) has been studied previously for the case in which one can ignore generic interactions with the substrate. The membrane was found to undergo lateral phase separation even for purely repulsive cis-interactions between the stickers if these stickers have an increased lateral size [18] or a larger bending rigidity than the lipid matrix [9]. The phase separation is then driven by the shape fluctuations of the membrane.

Here, we consider the interplay of the specific sticker potential (23) with a generic repulsive trans-interaction between the membrane and the substrate. If the range of these generic interactions is smaller than the potential range l_v of the stickers, the bound state of the stickers is more restricted, but the general entropic phase behavior described above will not be affected. However, for repulsive generic interactions with a potential range which exceeds l_v, a different scenario is possible. For simplicity, we consider here a generic potential of the form

$$V_g(l) = U_{ba}\theta(l_{ba} - l) = U_{ba}, \quad \text{for} \quad 0 \le l \le l_{ba},$$
$$= 0, \quad \text{for} \quad l > l_{ba}, \tag{24}$$

with a barrier height $U_{ba} > 0$ and range $l_{ba} > l_v$. The effective potential (6) obtained after the summation of the sticker degrees of freedom is shown in Figure 6 and can be
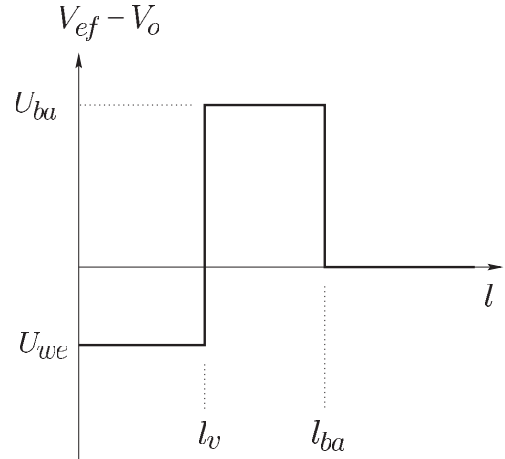
Fig. 6. Schematic form of the effective potential $V_{ef} - V_0$ defined in (25) as a function of the membrane separation l. The effective potential exhibits i) a potential barrier of height U_{ba} which extends up to the separation l_{ba}, see (24), and ii) a potential well which has the range l_v, arising from the short-ranged sticker potential (23), and the effective depth U_{we} as given by (26).

written as

$$V_{ef}(l) - V_0 = U_{we}, \quad \text{for} \quad 0 < l < l_v,$$
$$= U_{ba}, \quad \text{for} \quad l_v < l < l_{ba},$$
$$= 0, \quad \text{for} \quad l_{ba} < l, \tag{25}$$

with

$$U_{we} = U_{ba} - T\ln\frac{1 + e^{(\mu - U)/T}}{1 + e^{\mu/T}} \tag{26}$$

and the constant term $V_0 = -T\ln\left(1 + e^{\mu/T}\right)$ which depends only on the reduced chemical potential μ/T. Since the sticker binding energy U is negative, we have $U_{we} < U_{ba}$.

In the context of interacting membranes, an effective potential of the form (25) was first studied in reference [16]. More recently, such an interaction potential has also been derived for membranes which contain both stickers and repellers, *i.e.* non-adhesive molecules which protrude from the membrane surface [9]. The repellers have been modeled by a local square-barrier potential, the stickers by the local square-well potential (23). The generic square-barrier potential (24) thus affects the phase behavior in a similar way as repellers with a local square-barrier potential. As previously discussed, the membrane unbinds at a certain critical depth U_{we}^* of the attractive potential well which is given by [16]

$$|U_{we}^*| = ca^2T^2/\kappa l_v^2, \tag{27}$$

where c is a dimensionless coefficient, because the excess free energy for a membrane confined to a potential well with depth U_{we} is $V_{fl}(l_v) \sim T^2/\kappa l_v^2$, and the free-energy difference between the bound and the unbound state of the membrane reads $\Delta F = -|U_{we}|/a^2 + cT^2/\kappa l_v^2$. The character of the unbinding transition depends on the height of

the potential barrier which induces a line tension between bound and unbound membrane segments. On small length scales, this line tension can be estimated as $U_{\text{ba}}^{\text{eff}} L$ with effective barrier height $U_{\text{ba}}^{\text{eff}} = U_{\text{ba}} + |U_{\text{we}}| - cT^2/\kappa l_{\text{v}}^2$ and effective width $L \sim (l_{\text{ba}} - l_{\text{v}})\sqrt{\kappa/T}$ of the membrane strip crossing the barrier [16]. Taking also into account the line entropy on larger length scales, the unbinding transition is found to be discontinuous for relatively strong barriers with

$$U_{\text{ba}}(l_{\text{ba}} - l_{\text{v}})^2 \gg |U_{\text{we}}^*|l_{\text{v}}^2 \qquad (28)$$

and continuous for weak barriers with $U_{\text{ba}}(l_{\text{ba}} - l_{\text{v}})^2 \ll |U_{\text{we}}^*|l_{\text{v}}^2$. A discontinuous transition implies the coexistence of a bound phase with a high concentration of stickers and an unbound phase with a low sticker concentration. Therefore, sufficiently strong barriers also lead to lateral phase separation and sticker aggregation.

In contrast to the entropic mechanisms mentioned above, the phase separation is caused by the line tension between bound and unbound membrane patches. This line tension is induced by the potential barrier. In order to understand the influence of membrane fluctuations, we have to take into account that the transition value $|U_{\text{we}}^*|$ of the contact energy increases with the temperature T and decreases with the bending rigidity κ, see (27). As implied by (28), membranes with more pronounced shape fluctuations require larger potential barriers for a discontinuous unbinding transition and lateral phase separation. As in the first case studied in the previous section, membrane fluctuations decrease the tendency of the membrane to phase-separate.

5 Conclusions

In this article, we have studied one possible mechanism for adhesion-induced phase separation of biomimetic membranes. The mechanism is applicable to membranes which experience both specific attractive and generic repulsive trans-interactions. The specific interactions are taken to arise from sticker molecules which are embedded in the membrane, while the generic repulsion may originate, *e.g.*, from electrostatic forces between similarly and homogeneously charged membranes. The effective trans-interaction obtained by an explicit summation of the sticker degrees of freedom in the partition function is shown to exhibit a potential barrier. This barrier induces a line tension between bound and unbound membrane regions resulting in a coexistence of a sticker-rich phase, characterized by a small separation between membrane and substrate, and a sticker-poor phase, characterized by a larger membrane-substrate separation. Thermally excited shape fluctuations of the membrane are shown to decrease the tendency for lateral phase separation by reducing the potential barrier height.

Two different cases have been considered here. In the first case, the generic trans-interaction between membrane and substrate is assumed to have a minimum at a finite membrane separation and is approximated by a harmonic

potential centered at the minimum. The specific trans-interaction of the stickers is taken to depend linearly on membrane separation. This model introduced in reference [19] has been studied using a mean-field approach. The adhesion was shown to shift the critical point of the lateral phase transition. In the present article, the concentration field n of the stickers is described as a lattice gas variable on a discretized elastic membrane. The phase behavior is determined exactly in the absence of shape fluctuations of the membrane. Fluctuations of the membrane are subsequently taken into account by Monte Carlo simulations.

In the second case, the specific sticker trans-interaction is modeled by a short-ranged square-well potential, and the generic trans-interaction between membrane and substrate is assumed to be a purely repulsive step function. This second case turns out to be closely related to biomimetic membranes which contain stickers *and* repellers, *i.e.* repulsive molecules which protrude from the membrane surface [9], since the effective potential has the same functional form as in equation (25) and exhibits a potential barrier. As shown in references [16,17], the membrane fluctuations can "tunnel" through a relatively small barrier but are trapped by a relatively large one.

The mechanism for adhesion-induced phase separation as studied in the present article is distinct from several *entropic* mechanisms which have been identified in previous works [9,18]. Examples of these other mechanisms include stickers with an increased lateral size [18], stickers with an increased rigidity, and stickers with attractive cis-interactions which are renormalized by the shape fluctuations of the membrane [9]. These entropic mechanisms depend strongly on the rescaled potential range $(l_{\text{v}}/a)\sqrt{\kappa/T}$ of the stickers where l_{v} is the range of the square-well potential (23), and a is the size of the membrane patches. Thus, for the entropic mechanisms, the tendency for lateral phase separation *increases* with decreasing potential range and/or increasing temperature. This is in contrast to the mechanism described in the present work which is governed by the potential barrier contained in the effective interaction potential of the membrane. In this case, the shape fluctuations of the membrane reduce the potential barrier which implies that the tendency for lateral phase separation *decreases* with increasing temperature.

Experimentally, the temperature-dependence of adhesion-induced phase separation has not yet been studied. The presence of repulsive lipopolymers in the biomimetic systems investigated in references [12–15] points towards a barrier-mechanism for adhesion-induced phase separation as emphasized in this article. Entropic mechanisms, on the other hand, might be relevant in the case of membranes containing oppositely charged lipids [10,11] which induce a tight membrane coupling and small membrane separations below 4 nm [11].

References

1. R. Lipowsky, E. Sackmann (Editors), *Structure and dynamics of membranes: Generic and specific interactions*, Vol. **1B** of *Handbook of Biological Physics* (Elsevier, Amsterdam, 1995).
2. W. Helfrich, Z. Naturforsch. **33a**, 305 (1978).
3. R. Lipowsky, S. Leibler, Phys. Rev. Lett. **56**, 2541 (1986).
4. G.I. Bell, Science **200**, 618 (1978); G.I. Bell, M. Dembo, P. Bongrand, Biophys. J. **45**, 1051 (1984); G.I. Bell, in *Physical Basis of Cell-Cell Adhesion*, edited by P. Bongrand (CRC Press, Boca Raton, 1988) p. 227.
5. J. Braun, J.R. Abney, J.C. Owicki, Nature **310**, 316 (1984); J. Braun, J.R. Abney, J.C. Owicki, Biophys. J. **52**, 427 (1987).
6. R. Bruinsma, M. Goulian, P. Pincus, Biophys. J. **67**, 746 (1994).
7. B. Alberts *et al.*, *Molecular Biology of the Cell*, 3rd edition (Garland, New York, 1994).
8. R. Lipowsky, Phys. Rev. Lett. **77**, 1652 (1996).
9. T.R. Weikl, R. Lipowsky, Phys. Rev. E **64**, 011903 (2001).
10. J. Nardi, T. Feder, R. Bruinsma, E. Sackmann, Europhys. Lett. **37**, 371 (1997).
11. A.P. Wong, J.T. Groves, J. Am. Chem. Soc. **123**, 12414 (2001).
12. A. Albersdörfer, T. Feder, E. Sackmann, Biophys. J. **73**, 245 (1997).
13. A. Kloboucek, A. Behrisch, J. Faix, E. Sackmann, Biophys. J. **77**, 2311 (1999).
14. Z. Guttenberg, B. Lorz, E. Sackmann, A. Boulbitch, Europhys. Lett. **54**, 826 (2001).
15. C.W. Maier, A. Behrisch, A. Kloboucek, D.A. Simson, R. Merkel, Eur. Phys. J. E **6**, 273 (2001).
16. R. Lipowsky, J. Phys. II **4**, 1755 (1994).
17. A. Ammann, R. Lipowsky, J. Phys. II **6**, 255 (1996).
18. T.R. Weikl, R.R. Netz, R. Lipowsky, Phys. Rev. E **62**, R45 (2000).
19. S. Komura, D. Andelman, Eur. Phys. J. E, **3**, 259 (2000).
20. R. Bruinsma, A. Behrisch, E. Sackmann, Phys. Rev. E **61**, 4253 (2000).
21. R. Goetz, G. Gompper, R. Lipowsky, Phys. Rev. Lett. **82**, 221 (1999).
22. P.B. Canham, J. Theor. Biol. **26**, 61 (1970).
23. W. Helfrich, Z. Naturforsch. **28c**, 693 (1973).
24. R. Lipowsky, Europhys. Lett. **7**, 255 (1988).
25. K. Binder, D.W. Heermann, *Monte Carlo Simulations in Statistical Physics* (Springer, Berlin, 1992).